A Comparison of Integrated Water Vapor Sensors: WVIOP-96

J. C. Liljegren
Pacific Northwest National Laboratory
Richland, Washington

E. R. Westwater and Y. Han
NOAA/Cooperative Institute for Research in the Environmental Sciences (CIRES)
University of Colorado
Boulder, Colorado

Introduction

The 1996 Water Vapor Intensive Operations Period (WVIOP-96) was conducted at the Southern Great Plains (SGP) Cloud and Radiation Testbed (CART) central facility in September in order to assess the skill of a wide variety of sensors in measuring atmospheric water vapor.

Here we present a comparison of radiometric brightness temperatures (TB) and vertically-integrated or "precipitable" water vapor (PWV) amounts derived from eight collocated ARM microwave radiometers, as well as microwave radiometers from the National Oceanic and Atmospheric Administration (NOAA) Environmental Technology Laboratory (ETL) and the Microwave Remote Sensing Laboratory (MRSL) at the University of Massachusetts-Amherst. We also compare these PWV amounts with integrated ARM radiosondes and PWV derived from the propagation delay of radio signals using Global Positioning System (GPS) receivers deployed at the NOAA wind profiler radar in nearby Lamont, Oklahoma by the NOAA Forecast Systems Laboratory (FSL) and at the SGP CART central facility by the National Center for Atmospheric Research (NCAR). The GPS data were processed by the University NAVSTAR Consortium (UNAVCO) using the "Bernese" software. Comparisons were also carried out against PWV derived from the ARM multifilter rotating shadowband radiometer (MFRSR) sunphotometer by State University of New York (SUNY)-Albany.

Discussion

The basic quantity measured by microwave radiometers is the radiometric brightness temperature, which is directly proportional to the amount of microwave energy incident upon the antenna. From these measurements, the amount of water vapor directly overhead of the instrument is derived using a statistical retrieval technique. Differences in measured TB and derived PWV between each instrument and ARM radiometer "C1" are presented in Figure 1. Statistics are listed in Tables 1, 2, and 3.

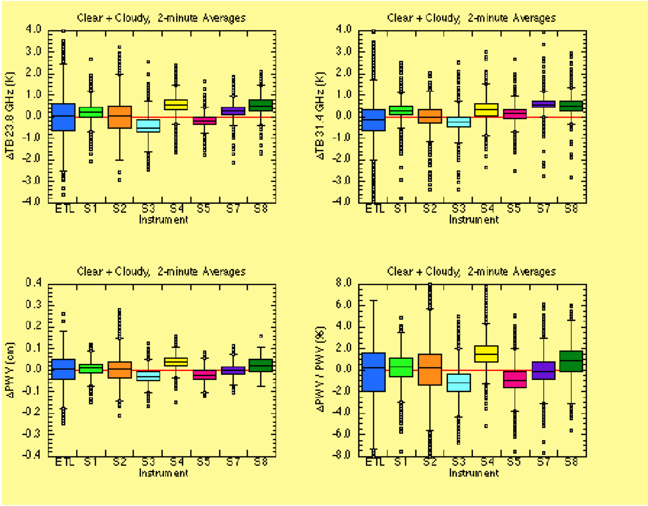

Figure 1. Box plots of differences of 2-minute averages of TB and PWV for non-precipitating conditions. The box encloses 50% of the data; the line inside the box indicates the median. The vertical lines enclose 100% of the data; the circles above and below indicate statistical outliers. The outliers are due to broken cloud fields transiting the radiometers' fields of view at slightly different times. The Liebe-87 model was used to predict the TB at the ARM frequencies from those measured with the ETL radiometer.

Table 1. Microwave radiometers at WVIOP-96.				
Organization	**Frequencies (GHz)**	**ID**	**S/N**	**Contact**
ARM SGP CF	23.8, 31.4	C1	10	Jim Liljegren
ARM SGP	23.8, 31.4	S1	11	Jim Liljegren
ARM SGP	23.8, 31.4	S2	04	Jim Liljegren
ARM SGP	23.8, 31.4	S3	12	Jim Liljegren
ARM SGP	23.8, 31.4	S4	19	Jim Liljegren
ARM SGP	23.8, 31.4	S5	15	Jim Liljegren
ARM SGP	23.8, 31.4	S7	20	Jim Liljegren
ARM SGP	23.8, 31.4	S8	21	Jim Liljegren
NOAA ETL	20.6, 31.65	ETL	-	Ed Westwater
UMASS MRSL	22.235, 23.835, 25.435, 27.035, 36.500	MRSL	-	Tim Sheve

Table 2. Additional PWV sensor at WVIOP-96.			
Organization	**Instrument**	**ID**	**Contact**
NOAA FSL	GPS at Lamont	GSP/LMT	Seth Gutman
NCAR	GPS at CF	GSP/CF	Dave Parsons
SUNY - Albany	Sunphotometer	MFRSR	Joe Michalsky
ARM SGP	Radiosonde	BBSS	Barry Lesht

Comparisons of PWV from the ARM-C1 and ETL radiometers and the GPS receiver at Lamont, Oklahoma are presented in Figure 2. The differences between radiometers and GPS must be borne in mind when considering these comparisons: the radiometers have a relatively high temporal and spatial resolution (2-3 samples per minute and a field of view of 2-5 degrees), whereas the GPS represents a 30-minute average along the paths to 4-5 GPS satellites as

Table 3. 2-Minute average brightness temperatures compared to ARM-C1.									
		23.8 GHz				**31.4 GHz**			
S1	11,871	1.012	-0.27	0.23	0.42	1.011	0.03	0.28	0.41
S2	11,332	0.987	0.59	0.02	0.74	0.979	0.45	-0.02	0.41
S3	11,245	0.999	-0.36	-0.43	0.59	1.008	-0.42	-0.24	0.42
S4	9,001	1.004	0.40	0.56	0.67	0.996	0.40	0.31	0.52
S5	9,853	0.991	0.20	-0.18	0.32	0.995	0.23	0.12	0.33
S7	10,543	1.008	-0.02	0.30	0.42	1.015	0.22	0.56	0.61
S8	10,575	1.018	-0.24	0.52	0.61	1.018	0.15	0.54	0.67
ETL	11,109	1.055	-2.4	0.02	0.81	1.019	-0.58	-0.15	0.76
MRSL	126	0.949	1.6	0.13	0.66	No comparable channel			

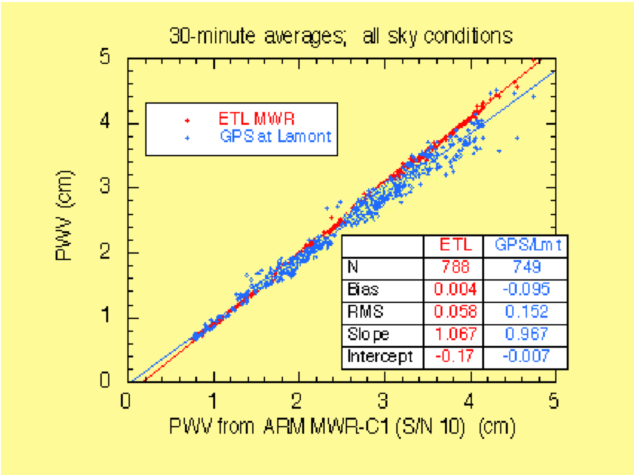

Figure 2. 30-minute averaged PWV from the ETL microwave radiometer and the GPS receiver at Lamont compared with the ARM-C1 radiometer.

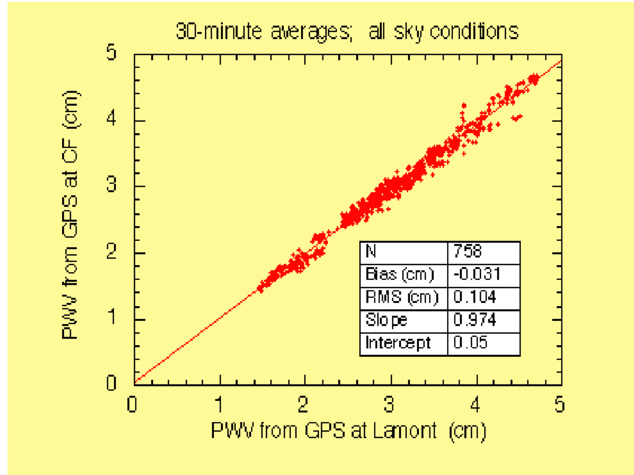

Figure 3. Comparison of PWV from the GPS receivers at Lamont and the SGP central facility.

they orbit the Earth. The scatter plot of 30-minute averages in Figure 2 shows that the radiometers were more highly correlated with each other than with the GPS. However, the slope between the GPS and ARM-C1 is close to unity, whereas the slope of the two radiometers is considerably different than unity. This arose from ETL's application of a constant calibration factor rather than one which varied in time according to the instrument variations. A time-varying calibration is being developed by ETL to address this variation.

The scatter plot of the results from the two GPS receivers also shows a near-unity slope but more scatter than between the two radiometers (Figure 3). Although the two GPS receivers were about 5 km apart, the scatter is believed to primarily result from differences in antenna type and "multi-path" errors (wherein the radio signals from the satellites reflect off the ground or other object rather than proceeding directly to the receiver).

A scatter plot of PWV from Vaisala RS-80 radiosondes compared with the ARM-C1 radiometer is presented in Figure 4. These reveal that radiosondes from a June calibration lot (serial numbers beginning with "62") and an August calibration lot (serial numbers beginning with "63") performed very differently. These results were confirmed by balloon ascents with two sondes, one from each calibration lot, on the same balloon.

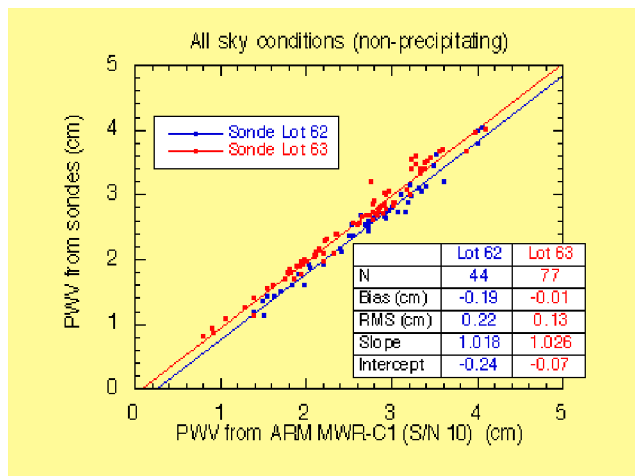

Figure 4. Radiosondes from June (lot 62) and August (lot 63) calibration lots compared with the ARM-C1 radiometer.

A comparison of PWV derived from a sunphotometer (the MFRSR) with that from radiometer ARM-C1 is presented in Figure 5. Because the sunphotometer tracks the sun, it samples the atmosphere along a different line-of-sight path than the radiometer. Consequently, horizontal variations in water vapor can result in different values of PWV reported by the two instruments. However, PWV determined near solar noon agreed very well with the radiometer.

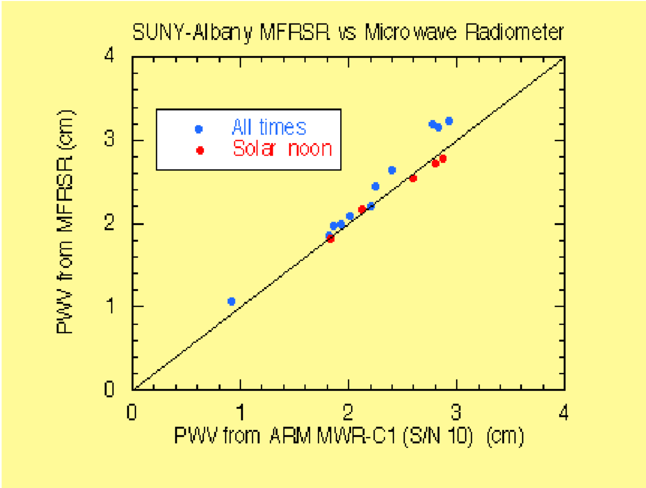

Figure 5. PWV from the MFRSR sunphotometer compared with the ARM-C1 radiometer. Agreement at solar noon (red) is usually good; agreement at other times (blue) depends on the degree to which the water vapor distribution is horizontally homogeneous.

Conclusions

The ARM microwave radiometers demonstrated excellent agreement (within 2-3%) over a wide range of TB and PWV under clear and cloudy skies.

The ETL radiometer was well-correlated with the ARM radiometers; its constant calibration value did not adequately account for instrument variations. Once these are accounted for by a time-varying calibration, the agreement with the ARM radiometers will improve.

The agreement between the radiometers and the GPS-retrieved PWV is good considering the temporal and spatial sampling differences between the two instrument systems.

The two radiosonde calibration lots exhibited large (7%) offsets in water vapor.

The sunphotometer was in good agreement with the microwave radiometer when it sampled along approximately the same line-of-sight path.